Longer Living Majority than Minority Image State at Fe(110)

F. Passek, M. Donath, K. Ertl, and V. Dose

Max-Planck-Institut für Plasmaphysik, EURATOM Association, D-85740 Garching bei München, Germany

(Received 2 May 1995)

A strongly spin-dependent lifetime is reported for the $n = 1$ image-potential surface state at Fe(110). Spin-resolved inverse photoemission measurements reveal an intrinsic linewidth of 140 ± 10 meV for the minority image state, about twice as large as the 70 ± 10 meV observed for the majority state. The spin dependence of the lifetime can be explained in terms of the spin-dependent density of bulk electronic states in iron, on the assumption that escape into bulk states accompanied by electron-hole-pair production is the main decay channel. The binding energies are magnetically split by 57 ± 5 meV. This result supports the predicted predominant influence of the spin-polarized substrate potential on the binding energy, modified by a small effect of the spin-polarized surface barrier.

PACS numbers: 73.20.At, 75.30.Pd, 79.60.Bm

Image-potential-induced surface states (IS's) in front of ferromagnetic surfaces are useful probes in at least two aspects. First, their spin-dependent binding energies provide information on the boundary conditions characterizing the "electron trap": the spin-dependent edges of the bulk band gap on the crystal side and the surface barrier towards the vacuum. Second, their lifetimes afford an insight into the nature of spin-dependent, inelastic processes right at and in front of a ferromagnetic surface.

IS's have their origin in the Coulomb attraction between an electron in front of a conductive surface and its own image charge in the solid [1]. Provided the reflectivity of the surface is high, i.e., there are no bulk states present to which the electron can couple, which is true in the case of a bulk band gap, the electron may be trapped between the bulk crystal barrier and the image-potential surface barrier. Because of the long-range nature of the Coulomb potential, this gives rise to a Rydberg-like series of bound states, the IS's, with wave functions peaked a few angstroms outside the topmost atomic layer.

Experimentally, IS's were first identified by inverse photoemission (IPE) [2]. Two-photon photoemission (2PPE) with its superior energy resolution succeeded in resolving several members of the Rydberg series and determining their intrinsic lifetimes [3]. Since the magnetic exchange splitting of IS's at ferromagnetic transition metals turned out to be smaller than the intrinsic lifetime broadening, the splitting was not accessible to 2PPE. It was again IPE, now in its spin-resolved mode, that allowed detection of exchange-split IS's at ferromagnetic samples [4–7]. The first unambiguous result on a clean ferromagnetic sample, the observed exchange splitting of 18 ± 3 meV for the $n = 1$ IS at Ni(111) [6], was interpreted as a consequence of the spin-split band-gap boundaries, i.e., a spin-dependent barrier height on the crystal side. It was concluded that the influence of a possibly spin-dependent image-potential barrier may be negligible, but no quantitative result could be given. A more favorable case, the IS's at Fe(110) with its larger exchange splitting (Fig. 1), was discussed in a theoretical paper [8]. It was stated that the spin splitting of IS's is the net result of two effects: the influences of the crystal and image barriers. The surprising result was that the two contributions have opposite sign (63 vs -14 meV for the $n = 1$ IS). The two competing effects lead to exchange splitting of 55 meV in a self-consistent calculation. Concerning the spin dependence of lifetimes, as far as we know, no experimental or theoretical result is available so far. In this Letter, we present spin-resolved IPE results on both binding energies and lifetimes of IS's at Fe(110).

The experimental setup for spin-resolved IPE and details about the measurement are published elsewhere [9,10]. Spin-polarized electrons from a GaAs photocathode impinge as a parallel beam with a divergence of less than 2° on a sample and undergo radiative transitions into empty states. The emitted photons are detected in an energy-selective Geiger-Müller counter ($\hbar\omega = 9.4$ eV). The sample was a 15-monolayer-thick bcc Fe film de-

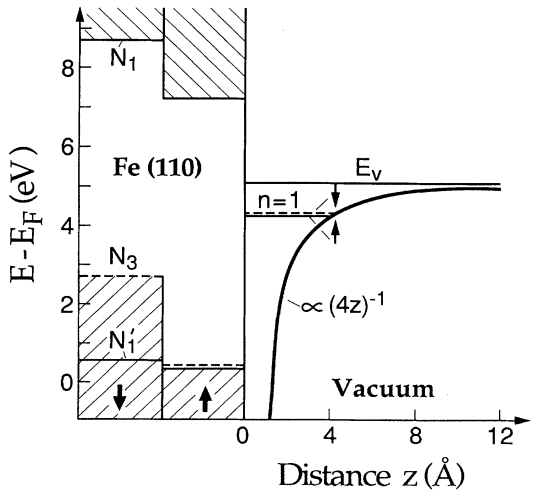

FIG. 1. Schematic potential diagram for IS's at Fe(110) indicating the image-potential barrier outside the crystal and the bulk sp band gap between $N_{1'}$ and N_1, including the uppermost d band of symmetry N_3.

 0031-9007/95/75(14)/2746(4)$06.00

posited on W(110). The films were prepared by evaporation from an Fe stick heated by electron bombardment at a pressure in the vacuum chamber of 3×10^{-10} mbar. The temperature of the substrate was kept at 270 K during deposition of the first 5 monolayers (ML) and increased to 550 K for the following 10 ML. The first 2 ML of Fe grow pseudomorphically on W(110). During further growth the lattice misfit between Fe and W of approximately 10% is overcome by lattice displacements until, at a thickness of about 10 ML, bcc Fe grows with its own lattice constant [11]. 15-ML films exhibit an electronic structure characteristic of bcc Fe(110) [12]. The good surface quality of our films is convincingly proved by the intensity of the IS emission. In addition, the structure and purity of the films were controlled by Auger electron spectroscopy and low-energy electron diffraction. For reasons of cleanliness, about every 50 min a new Fe film had to be prepared by flashing the tungsten to 2300 K and renewed Fe evaporation. About 100 single spectra from 16 film preparations were checked and then accumulated to get the statistics needed (up to 106 000 counts per point). The Fe films were remanently magnetized by a current pulse through a magnetization coil. The magnetic field was applied in the film plane along $[1\bar{1}0]$, the direction of easy magnetization for bcc Fe films in this thickness range [13]. Single-domain magnetization was proved by *extra situm* Kerr microscopy and by the squareness of hysteresis loops from *in situ* Kerr magnetometry. All IPE data were recorded at room temperature.

Figure 2 shows IPE data for normal incidence on Fe(110). On top of a spin-dependent linear background there appears a strong spectral feature at about 4.4 eV above the Fermi energy E_F, originating from transitions into the $n = 1$ IS. The steplike increase at the high-energy side of the peak represents the unresolved $n = 2, 3, \ldots$ members of the Rydberg series below the vacuum level E_V and the continuum states above it. The spin-resolved data of Fig. 2(a) reveal magnetic exchange splitting which becomes even clearer in Fig. 2(b), where an enlarged energy scale is used and the peak maxima are normalized by adding a constant offset to the majority data. A quantitative value for the exchange splitting is deduced from a least-squares fitting procedure described in detail elsewhere [6]. The best fit is shown in Fig. 2(b) as a solid line through the data points. The magnetic exchange splitting of the $n = 1$ IS at Fe(110) is determined at 57 ± 5 meV.

Theoretical considerations within the one-step model of IPE gave a lower limit of 30 meV for the exchange splitting [14]. Depending on the position of the image plane, however, this calculation expected splittings of up to 100 or 200 meV. Calculations within the phase-shift model estimated a splitting of 27 meV [15]. In both cases the surface barrier was assumed to be spin independent. On the basis of 2PPE results, an upper limit of 80 meV for the exchange splitting was deduced [16]. The most sophisticated calculation so far was carried out by spin-polarized near-surface embedding [8]. The result of 55 meV for the $n = 1$ IS, primarily caused by coupling to the spin-polarized substrate potential and reduced by the spin-polarized surface barrier, is in excellent accord with our experimental value of 57 ± 5 meV. The agreement may be taken as strong support for the conclusion of the calculation, viz. the effect of the spin-polarized surface barrier on IS's at Fe(110) is relatively small and opposite in sign to the substrate contribution.

IS's are long-living electronic states in relation to other empty bulk or surface states, because their wave functions are peaked a few angstroms in front of the surface, i.e., the overlap with other states is small. Decay into bulk or surface states via electron-hole-pair production, also called Auger and surface Auger processes, is assumed to dominate the relaxation dynamics [17,18]. Energy-resolved [3] as well as time-resolved experiments [19] report lifetimes of 5 to 30 fs, corresponding to linewidths of 130 to 20 meV for the $n = 1$ IS. Model calculations using free-electron-like bulk states and taking account of the penetration of the IS wave function into the solid yield linewidths of the order of some tens of meV [17]. The penetration strongly depends on the energetic position of the IS relative to the band gap. This explains the increased linewidth of IS's close to band-gap boundaries. The influence of surface states on the relaxation dynamics is still the subject of debate [18]. A slight decrease in linewidth for the $n = 1$ IS on Ni(111) by surface-state quenching has been reported [20]. Considering (i) the penetration of the wave function and (ii) the influence of surface states turns out to be insufficient to explain the observed large IS linewidths at the ferromagnetic $3d$ metals Ni and Fe: 70 ± 8 meV for Ni(001), 84 ± 10 meV for Ni(111) [20], and 130 ± 30 meV for Fe(110) [16]. The small magnetic exchange splittings of 13 ± 13 meV [5], 18 ± 3 meV [6], and 57 ± 5 meV, respectively, cannot account for the linewidths observed by spin-integrated 2PPE. While the existence of an empty surface state at Ni(111) [21] may explain the slightly larger linewidth at Ni(111) in relation to Ni(001), what causes the broadening at Ni(001) compared with 21 ± 4 meV at Ag(001) and 28 ± 6 meV at Cu(001) [3]? All three IS's have about the same energetic position relative to the band gap. The most severe shortcoming of the models described is that they ignore the individual band structure of the material, in the case of Ni and Fe the large density of empty d states. One more question has not been addressed so far: Is the lifetime spin dependent?

Comparing the line shapes in Figs. 2(a) and 2(b) reveals a larger peak width combined with a smaller peak maximum for the minority in relation to the majority channel. Because of the limited energy resolution of IPE, the observed linewidth reflects primarily the apparatus function rather than the lifetime broadening. Nevertheless, the significantly different linewidths in the two spin channels indicate a spin-dependent lifetime. Since we know, from a maximum entropy analysis, that a Gaussian func-

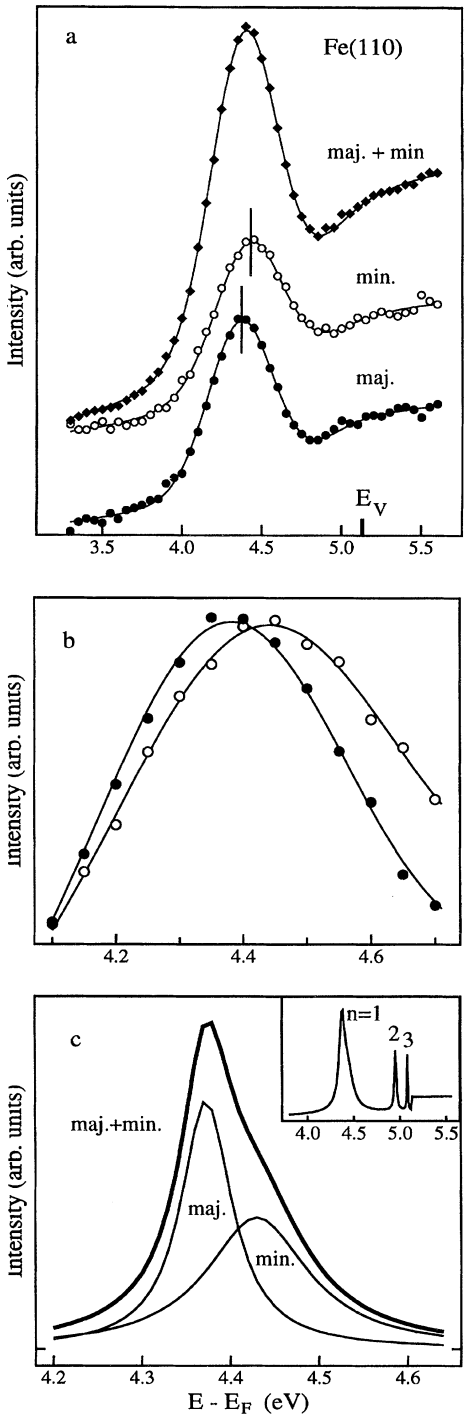

FIG. 2. (a) Spin-resolved and spin-integrated IPE results (normal electron incidence) of image states at Fe(110). (b) Same spin-resolved data on an enlarged energy scale and with the peak maxima normalized by adding a constant offset to the majority data. (c) Spin-resolved and spin-integrated intrinsic line shapes of the $n = 1$ IS, with the background subtracted. Inset: Components of the best fit curve ($n = 1, 2, 3$ states plus background, spin integrated).

tion with FWHM = 460 meV is a fairly good approximation to the apparatus function [22], we are able to derive the intrinsic linewidth by a simulation approach. Artificial spectra were generated by composition of a linear background with a steplike increase at E_V and three Lorentzian functions representing the first three members of the IS series, followed by convolution with the apparatus function. The spin-dependent energy positions of the $n = 1$ IS were taken from our data, the binding energies for the $n = 2, 3$ members from 2PPE [16]. The linewidths of the latter two states were taken as spin independent with values of 25 and 10 meV for the $n = 2$ [16] and $n = 3$ states, respectively. Ignoring any spin dependence of the $n = 2, 3$ states is a reasonable approximation, because with increasing n the IS are localized further away from the ferromagnetic surface and their spectral weight decreases significantly. Parameters of the simulation are the intrinsic linewidths of the $n = 1$ states, the amplitudes of all Lorentzians, the linear background, and the step height. The solid lines through the data points in Fig. 2(a) represent the best fit to the data with intrinsic linewidths of 140 and 70 meV for the minority and majority channels, respectively. Changing the linewidths by more than 10 meV results in a significantly worse agreement between the data and simulation. As a result of the simulation, Fig. 2(c) shows the intrinsic line shapes, without background, step function, and convolution with the apparatus function. The various components for the spin-integrated case are given in the inset. A similar approach was used to deduce the spin-integrated linewidth of 130 $\pm$ 30 meV from 2PPE results [16]. Our spin-integrated result is somewhat asymmetric, nevertheless the FWHM of 125 meV is in good agreement with the 2PPE result, where only one Lorentzian was used. Additional confidence in our simulation approach comes from the fact that the integral intensity is the same within 3% in both spin channels. The remarkable result of our measurement is that the majority $n = 1$ IS at Fe(110) lives about twice as long as its minority counterpart. The linewidths of 140 and 70 meV correspond to lifetimes of 4.7 and 9.4 fs, respectively.

A reanalysis of our data of Ni(111) [6] resulted in a, within 10 meV, spin-independent linewidth of 80 meV for the $n = 1$ IS. How can these quite different experimental findings for Ni and Fe be explained? The penetration of the wave function owing to the position of the IS within the band gap is certainly somewhat spin dependent in the Fe case, but cannot explain a factor of 2 in lifetime. Neither minority nor majority IS come close to the gap boundary, where the penetration significantly changes. In addition, no spin-dependent surface state has been detected that could influence the lifetime. The almost spin-independent lifetimes for Ni(111) even question the relevance of surface states to the relaxation dynamics in view of the magnetic surface state at E_F [21].

To learn more about the material and spin dependence of the lifetime, we calculated the probability of decay into bulk states via electron-hole-pair production by taking into

account the actual band structure of the material. The escape from an electronic state at energy E into bulk states depends on (i) the available empty bulk states of energy E' smaller than E, (ii) the number of occupied electron states, available for hole creation, with binding energy E_h smaller than or equal to the energy loss $\epsilon = E - E'$, and (iii) the number of empty states at $E_h + \epsilon$ available for the electron-hole excitation. We assume a constant matrix element for all transitions and take into account spin conservation within the deexcitation and excitation processes but no spin correlation between the two. With any wave-vector dependence being ignored, the spin-dependent transition rate is proportional to $W_{\uparrow,\downarrow}$, a convolution of the density of states ρ, in the following way:

$$W_{\uparrow,\downarrow}(E) = \int_0^E \rho_{\uparrow,\downarrow}(E') \Big(\int_{-\epsilon}^0 \rho_\uparrow(E_h)\rho_\uparrow(E_h + \epsilon) + \rho_\downarrow(E_h)\rho_\downarrow(E_h + \epsilon)\, dE_h \Big) dE'.$$

The result of this convolution based on density-of-states calculations [23] is shown in Fig. 3 for Fe, Ni, and Cu. The energies of the $n = 1$ IS's are marked by vertical lines. As a first conclusion, the model calculations describe fairly well the increasing linewidth of the IS's from Cu, Ni, to Fe. This emphasizes the importance of the bulk band structure for understanding the relaxation dynamics of IS's. Secondly, the spin dependence of the decay rates is expected to be much larger for Fe than for Ni. This qualitative trend is also found in the experiment. Exact quantitative predictions cannot be expected from this simple model in view of the assumption made. Nevertheless, the model describes qualitatively the material as well as spin dependence of the lifetime of IS's. To develop a more detailed understanding of the relaxation dynamics of IS's, one has to consider several aspects: (i) the penetration of the wave function into the solid, (ii) the influence of surface states, and, as shown in this Letter, and (iii) the actual bulk band structure of the material.

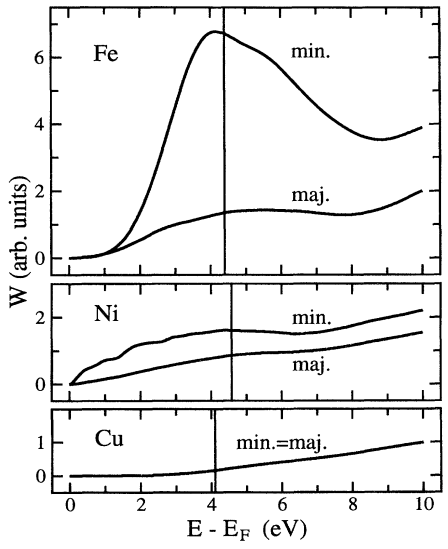

FIG. 3. Model calculations of $W_{\uparrow,\downarrow}(E)$, a quantity proportional to the spin-dependent probability of transitions into bulk states accompanied by electron-hole-pair production, for Fe, Ni, and Cu (see text for details). The energies of the $n = 1$ IS are marked by vertical lines.

We thank E. Bertel and A. Goldmann for helpful discussions. Financial support from the Deutsche Forschungsgemeinschaft is gratefully acknowledged.

[1] P. M. Echenique and J. B. Pendry, Prog. Surf. Sci. **32**, 111 (1990), and references therein.
[2] P. D. Johnson and N. V. Smith, Phys. Rev. B **27**, 2527 (1983); V. Dose *et al.*, Phys. Rev. Lett. **52**, 1919 (1984); D. Straub and F. J. Himpsel, *ibid.* **52**, 1922 (1984).
[3] Th. Fauster and W. Steinmann, in *Photonic Probes of Surfaces,* edited by P. Halevi (Elsevier, Amsterdam, 1995); S. Schuppler *et al.*, Phys. Rev. B **46**, 13 539 (1992).
[4] M. Donath and K. Ertl, Surf. Sci. Lett. **262**, L49 (1992).
[5] K. Starke, K. Ertl, and V. Dose, Phys. Rev. B **45**, 6154 (1992).
[6] F. Passek and M. Donath, Phys. Rev. Lett. **69**, 1101 (1992).
[7] S. Bode *et al.*, Phys. Rev. Lett. **72**, 1072 (1994).
[8] M. Nekovee, S. Crampin, and J. E. Inglesfield, Phys. Rev. Lett. **70**, 3099 (1993).
[9] U. Kolac *et al.*, Rev. Sci. Instrum. **59**, 1931 (1988).
[10] M. Donath, Surf. Sci. Rep. **20**, 251 (1994).
[11] M. Przybylski, I. Kaufmann, and U. Gradmann, Phys. Rev. B **40**, 8631 (1989).
[12] V. Dose and M. Glöbl, in *Polarized Electrons in Surface Physics,* edited by R. Feder (World Scientific, Singapore, 1985), p. 547.
[13] U. Gradmann, J. Korecki, and G. Waller, Appl. Phys. A **39**, 101 (1986).
[14] G. Borstel and G. Thörner, Surf. Sci. Rep. **8**, 1 (1988).
[15] F. J. Himpsel, Phys. Rev. B **43**, 13 394 (1991).
[16] R. Fischer *et al.*, Phys. Rev. B **46**, 9691 (1992).
[17] P. M. Echenique, F. Flores, and F. Sols, Phys. Rev. Lett. **55**, 2348 (1985); P. de Andrés, P. M. Echenique, and F. Flores, Phys. Rev. B **35**, 4529 (1987).
[18] S. Gao and B. I. Lundqvist, Prog. Theor. Phys. Suppl. **106**, 405 (1991); Solid State Commun. **84**, 147 (1992).
[19] R. W. Schoenlein *et al.*, Phys. Rev. B **43**, 4688 (1991).
[20] N. Fischer *et al.*, Phys. Rev. B **42**, 9717 (1990).
[21] M. Donath, F. Passek, and V. Dose, Phys. Rev. Lett. **70**, 2802 (1993).
[22] W. von der Linden, M. Donath, and V. Dose, Phys. Rev. Lett. **71**, 899 (1993).
[23] J. Noffke (private communication).